Journal of Electronic Research and Application, 2024, Volume 8, Issue 4
http://ojs.bbwpublisher.com/index.php/JERA
ISSN Online: 2208-3510
ISSN Print: 2208-3502

Research on Active and Reactive Power Decoupling Control Based on VSC-HVDC

Hongshan Lin, Yiming Lei, Feng Ning*

Department of Electric Power Engineering, North China Electric Power University, Baoding 071000, Hebei Province, China

***Corresponding author:** Feng Ning, ningfeng9909@163.com

Abstract: Voltage Source Converter-based High Voltage Direct Current (VSC-HVDC) transmission technology represents a groundbreaking approach in high voltage Direct Current (DC) transmission, offering numerous technical advantages and broad application prospects. However, in the d-q synchronous rotating coordinate system, the VSC-HVDC exhibits the coupling effect of active power and reactive power, so it needs to be decoupled. This paper introduces the basic principle and mathematical model of the VSC-HVDC transmission system. Through the combination of coordinate transformation and variable substitution, a feedforward decoupling control method is derived. Then the VSC-HVDC simulation model is designed, and the simulation analysis is carried out in the MATLAB environment. The simulation results demonstrate that the method effectively achieves decoupling control of active and reactive power, exhibiting superior dynamic performance and robustness. These findings validate the correctness and effectiveness of the control strategy.

Keywords: Voltage source converter; Decoupling control; Feedforward decoupling

Online publication: August 13, 2024

1. Introduction

VSC-HVDC has the characteristics of not being limited by transmission distance, independent control of active power and reactive power, and no risk of commutation failure [1–3]. With its unique technical advantages, it has become an important way to solve the problem of large-scale new energy delivery and a powerful means to adjust the energy structure in the future [4–6].

In a previous study, the steady-state VSC-HVDC model is analyzed, alongside proposing a PI-based nonlinear controller [7]. Yet, the interplay among the relevant physical quantities described by the model is intricate, posing challenges in determining the controller parameters. By formulating the mathematical model of the synchronous rotating coordinate system of the voltage source converter station, previous studies implemented a nonlinear decoupling controller for active and reactive power based on feedback linearization [8,9]. This approach achieves independent and rapid control over the converter station‘s active and reactive power outputs but does not discuss the power control in depth. Peng proposed to use the internal model principle to

design the controller of VSC-HVDC, though it did not specify the foundational indices for tuning the internal model controller parameters [10].

In summary, the research on the decoupling control strategy of the VSC-HVDC system is mainly aimed at the decoupling between the output active and reactive power of the converter station, and the detailed design method of the inner and outer loop controller but the basis index of the internal model controller parameters setting was not given.

This paper presents the fundamental principles and mathematical model of VSC-HVDC transmission systems. Through the combination of coordinate transformation and variable substitution, a feedforward decoupling control method that can independently control active power and reactive power and can completely decouple them is derived. The inner loop controller design method and the fundamental parameters for tuning the internal model controller are provided. With internal model control relying solely on a filter time constant, the process of tuning controller parameters is straightforward. Simulation results affirm that the designed controller exhibits high-quality dynamics, robustness, and effective resistance to system disturbances and interference.

2. VSC-HVDC principle and mathematical model

Figure 1 shows the topology of the VSC-HVDC converter [11,12]. In **Figure 1**, R and L represent the equivalent reactance and loss resistance of the system, C represents the DC capacitance, and U_{sa}, U_{sb}, and U_{sc} represent the a, b, and c phase fundamental wave components of the symmetric Alternating Current (AC) system voltage. U_{ca}, U_{cb}, and U_{cc} are the a, b, and c phase fundamental components of the VSC AC voltage measurement. I_a, I_b, and I_c are fundamental components of the a, b, and c phases of AC measurement [13].

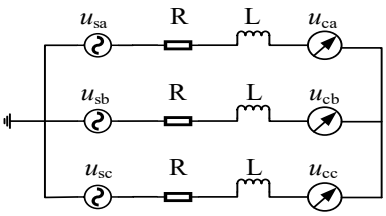

Figure 1. AC measurement equivalent circuit of the converter

According to Kirchhoff's Voltage Law (KVL), the transient mathematical model of the VSC-HVDC system on the VSC1 side in the abc three-phase stationary coordinate system is as follows:

$$\begin{cases} U_{sa} = L\dfrac{dI_a}{dt} + RI_a + U_{ca} \\ U_{sb} = L\dfrac{dI_b}{dt} + RI_b + U_{cb} \\ U_{sc} = L\dfrac{dI_c}{dt} + RI_c + U_{cc} \end{cases} \tag{1}$$

The mathematical model of the VSC-HVDC system established in the abc three-phase stationary coordinate system is a differential equation with time-varying coefficients, which is not conducive to the design of a high-performance controller. Therefore, it is necessary to analyze the d-q synchronous coordinate system: abc/d-q coordinate transformation matrix P is introduced [14]:

$$P=\frac{2}{3}\begin{bmatrix}\cos\theta & \cos(\theta-120°) & \cos(\theta+120°)\\ -\sin\theta & -\sin(\theta-120°) & -\sin(\theta+120°)\\ \frac{1}{2} & \frac{1}{2} & \frac{1}{2}\end{bmatrix} \tag{2}$$

There is no zero sequence component in the symmetric three-phase AC system, and the transient mathematical model of the commutator side in the d-q synchronous coordinate system can be obtained after the change:

$$\begin{cases} L_1\dfrac{di_{d1}}{dt}=u_{sd1}-u_{cd1}-\omega L_1 i_{q1}-R_1 i_{d1} \\ L_1\dfrac{di_{q1}}{dt}=u_{sq1}-u_{cq1}-\omega L_1 i_{d1}-R_1 i_{q1}\end{cases} \tag{3}$$

In the above formula, i_{d1} and i_{q1} represent the d-axis component and q-axis component of i_1, respectively. ω is the angular frequency of the AC system, taking ω = 2πf = 314 rad/s. u_{sd1} and u_{sq1} represent the d-axis component and q-axis component of u_{s1}, respectively. u_{cd1} and u_{cq1} represent the d-axis and q-axis components of u_{c1}, respectively.

3. Analysis of current decoupling control in inner loops

The loop controller accepts the reference value i_{dref} and i_{qref} of active and reactive current from the outer loop control and quickly tracks the reference current to realize the direct control of the current waveform and phase on the AC side of the converter. Inner loop control mainly includes inner loop current control, negative sequence voltage control, and Phae-Locked Loop (PLL) loop control. The following describes the inner loop current control strategy.

For the convenience of analysis, the VSC system function is obtained by Laplace transformation of **Equation (3)** as follows:

$$\begin{cases}(R+Ls)i_{vd}(s)=-u_{sd}(s)+u_{dref}(s)+\omega L i_{vq}(s)\\ (R+Ls)i_{vq}(s)=-u_{sq}(s)+u_{qref}(s)-\omega L i_{vd}(s)\end{cases} \tag{4}$$

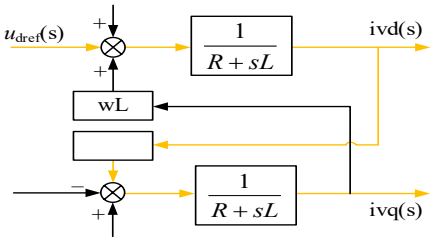

Figure 2. Program block diagram of VSC system function

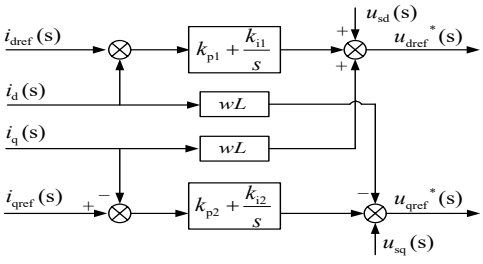

Figure 3. Current decoupling controller

It can be seen from **Figure 2** that the current of the d and q axes is affected not only by the control quantities u_{cd} and u_{cq}, but also by the current cross-coupling ωLi_{sd}, $\omega Li_{sq,}$ and the grid voltage u_{sd} and u_{sq}. To eliminate current coupling and grid voltage disturbance between the d and q axes, it is necessary to introduce

feedforward decoupling. Introduce intermediate variables $V_d(s)$ and $V_q(s)$, as follows:

$$\begin{cases} V_d(s) = \left[i_{dref}(s) - i_d(s) \right] \left(k_{p1} + \dfrac{k_{i1}}{s} \right) \\ V_q(s) = \left[i_{qref}(s) - i_q(s) \right] \left(k_{p1} + \dfrac{k_{i1}}{s} \right) \end{cases} \tag{5}$$

By substituting **Equation (4)** and **Equation (5)** into **Equation (3)**, then **Equation (6)** can be obtained, and the program block diagram is drawn as shown in **Figure 3**.

$$\begin{cases} U_{dref^*}(s) = u_{sd}(s) - \omega L i_q(s) + \left[i_{dref}(s) - i_d(s) \right] \left(k_{p1} + \dfrac{k_{i1}}{s} \right) \\ U_{qref^*}(s) = u_{sq}(s) - \omega L i_d(s) + \left[i_{qref}(s) - i_q(s) \right] \left(k_{p1} + \dfrac{k_{i1}}{s} \right) \end{cases} \tag{6}$$

Further analysis of **Figure 3** shows that after current decoupling control is adopted for the VSC converter, the d-axis and q-axis of its current controller become two independent control rings, that is, **Figure 4** can be simplified into the system structure shown in **Figure 5**.

This algorithm based on feedforward control makes the current inner loop in the mathematical model of voltage source converter realize decouple control, and the control of i_d and i_q are not affected by each other, and the dynamic performance of the system is improved by PI regulator, and the relevant current controller parameters can be easily designed to meet the requirements of the dynamic response speed of the system.

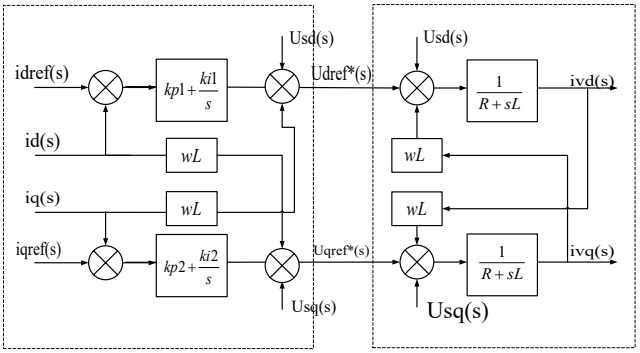

Figure 4. Internal model decoupling controller diagram of VSC system

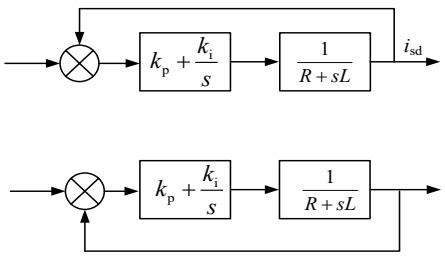

Figure 5. Simplified VSC converter station inner loop current control system structure diagram

4. Simulation analysis

Based on the MATLAB simulation platform, a three-phase, two-level, six-pulse, two-terminal VSC-HVDC system model was established. The main parameters are shown in **Table 1**.

A VSC-HVDC system model with active systems connected at both ends is established, and the parameters of the converter stations at both ends are consistent. Both the VSC1 side and the VSC2 side adopted the internal current loop. Because the reactive power is relatively small, only the VSC2 side adopts the control strategy of fixed DC voltage outer loop, and the VSC1 side directly sets the d-axis current reference value and the q-axis current reference value. Detailed control instructions are shown in **Table 2**.

Table 1. Major parameter

Parameter	Value
Frequency	50 Hz
Root Mean Square (RMS) of system 1 line voltage	220 kV
Short-circuit capacity ratio	10
Loss resistance	0.1 pu
Ac reactance	0.1 pu
Direct current capacitance	200 μF
Rated capacity of the converter station	300 MVA
Rated DC voltage	300 kV
Transformer connection mode	Yg/D1
Pulse Width Modulation (PWM) switching frequency	2600 Hz

Table 2. Major parameter

	Time (s)	1	1.5
1	I_{dref}	0.5→1	
	I_{qref}		0→0.2
2	V_{dcref}	1→1	
	I_{qref}		0→0

The simulation waveform of the sending end is the same as that of the single-ended VSC. We found that at the receiving end, at 1 s, P and i_d at the receiving end also decreased with the change of P at the sending end, because the active power at both ends was equal, and when the active power sent by the sending end was reduced, the active power at the receiving end would certainly be affected.

It can be concluded from **Figure 6** and **Figure 7** that the VSC-HVDC two-terminal model established in this paper realizes the decoupling control of the inner current loop well. The algorithm based on feedforward control makes the inner current loop realize the independent decoupling control of active and reactive power in the mathematical model of the voltage source converter so that the control of i_d and i_q do not affect each other.

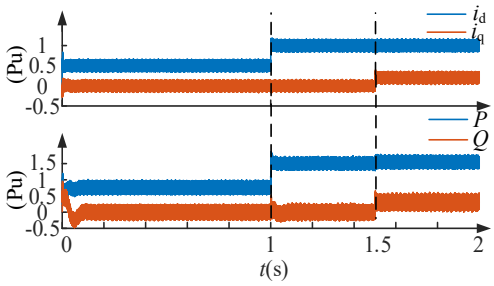

Figure 6. Send i_d, i_q and P and Q waveforms

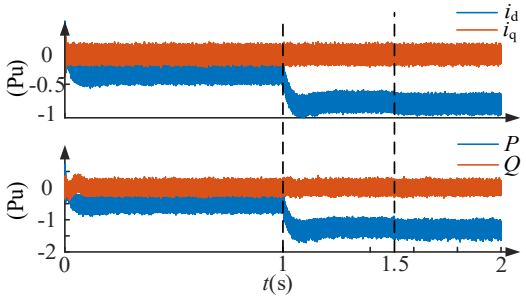

Figure 7. Receiver i_d, i_q and P and Q waveforms

5. Retrospect and prospect

This paper establishes the mathematical model of VSC-HVDC in both the abc three-phase stationary coordinate system and the d-q two-phase synchronous rotating coordinate system. Additionally, it analyzes the principles of VSC-HVDC direct current control. According to the mathematical model of VSC-HVDC in the d-q coordinate system, the feedforward decoupler is introduced by the principle of internal model control to decouple the inner current loop. Based on this theory, MATLAB is used to establish a simulation model for verification. The results indicate that the proposed scheme exhibits effective control performance. The designed controller demonstrates rapid response speed, enabling proficient active and reactive power decoupling control. Moreover, it showcases excellent tracking capabilities and robustness against external disturbances.

VSC-HVDC realizes the decoupling of active power and reactive power and has a good tracking effect and anti-interference ability. However, the switching state of the VSC-HVDC power electronic device submodule changes frequently, and the switching frequency of the VSC-HVDC power electronic device is high, which leads to its bad voltage balancing characteristic and large power loss. When the modular multilevel modulation technology is applied to the flexible DC transmission, that is, the AC voltage of the Modular Multilevel Converter (MMC) output is approximated to the modulated wave by investing and cutting out the submodules, which can meet the requirements of high voltage and high power. In this case, the harmonic problem is not serious, the stepped wave modulation can achieve good output characteristics, and its switching times are smaller than PWM, which can significantly reduce the switching loss. Later research work can also be further studied in MMC.

Disclosure statement

The authors declare no conflict of interest.

References

[1] Abedin T, Lipu MSH, Hannan MA, et al., 2021, Dynamic Modeling of HVDC for Power System Stability Assessment: A Review, Issues, and Recommendations. Energies, 14(16): 4829–4829.

[2] Garciarivas RS, Gonzalez DR, Navarro JA, et al., 2021, VSC-HVDC and its Applications for Black Start Restoration Processes. Applied Sciences, 11(12): 5648–5648.

[3] Li B, He J, Li Y, et al., 2019, A Review of the Protection for the Multi-Terminal VSC-HVDC Grid. Protection and Control of Modern Power Systems, 4(1): 1–11.

[4] Wu X, Xu Z, Zhang Z, 2021, Power Stability Analysis and Evaluation Criteria of Dual-Infeed HVDC with LCC-HVDC and VSC-HVDC. Applied Sciences, 11(13): 5847–5847.

[5] Sultan YA, Kaddah SS, Eladl AA, 2021, VSC-HVDC System-Based on Model Predictive Control Integrated with Offshore Wind Farms. IET Renewable Power Generation, 15(6): 1315–1330.

[6] Karami E, Gharehpetian BG, Mohammadpour H, et al., 2020, Generalised Representation of Multi-Terminal VSC-HVDC Systems for AC-DC Power Flow Studies. IET Energy Systems Integration, 2(1): 50–58.

[7] Xing C, Liu M, He X, et al., 2019, Research on Flexible Control Technology of HVDC. 2019 IEEE 8th International Conference on Advanced Power System Automation and Protection (APAP), Xi'an, China, 2019: 1186–1190.

[8] Gomis-Bellmunt O, Sau-Bassols J, Prieto-Araujo E, et al., 2020, Flexible Converters for Meshed HVDC Grids: From Flexible AC Transmission Systems (FACTS) to Flexible DC Grids. IEEE Transactions on Power Delivery, 35(1): 2–15.

[9] Chen Y, Moreno R, Strbac G, et al., 2018, Coordination Strategies for Securing AC/DC Flexible Transmission

Networks with Renewables. IEEE Transactions on Power Systems, 33(6): 6309–6320.

[10] Peng FZ, 2017, Flexible AC Transmission Systems (FACTS) and Resilient AC Distribution Systems (RACDS) in Smart Grid. Proceedings of the IEEE, 105(11): 2099–2115.

[11] Maza-Ortega JM, Acha E, Garcia S, et al., 2017, Overview of Power Electronics Technology and Applications in Power Generation Transmission and Distribution. Journal of Modern Power Systems and Clean Energy, 5(4): 499–514.

[12] Davari M, Mohamed YARI, 2016, Dynamics and Robust Control of a Grid-Connected VSC in Multiterminal DC Grids Considering the Instantaneous Power of DC- and AC-Side Filters and DC Grid Uncertainty. IEEE Transactions on Power Electronics, 31(3): 1942–1958.

[13] Kalari PY, Geetha RS, 2016, Performance Analysis of Paralleled VSC-HVDC Systems. 2016 International Conference on Microelectronics, Computing and Communications (MicroCom), Durgapur, India, 2016: 1–6.

[14] Rong M, Wu T, Li X, et al., 2020, Research on Grid Connection of Wind Farms Based on VSC-HVDC System. 12th IEEE PES Asia-Pacific Power and Energy Engineering Conference (APPEEC), Nanjing, China, 2020: 1–5.